Cavity ring-down spectroscopy sensor for ion beam etch monitoring and end-point detection of multilayer structures

Tao, Lei
Department of Mechanical Engineering, Colorado State University

Yalin, Azer P.
Department of Mechanical Engineering, Colorado State University

Yamamoto, Naoji
Department of Advanced Energy Engineering Science, Kyushu University

出版情報：Review of Scientific Instruments. 79, pp.115107-, 2008-11-18. AIP
バージョン：

Cavity ring-down spectroscopy sensor for ion beam etch monitoring and end-point detection of multilayer structures

L. Tao,[1] A. P. Yalin,[1,a)] and N. Yamamoto[2,b)]
[1]*Department of Mechanical Engineering, Colorado State University, Fort Collins, Colorado 80523, USA*
[2]*Department of Advanced Energy Engineering Science, Kyushu University, 6-1 Kasuga-kouen, Kasuga, Fukuoka 816-8580, Japan*

(Received 29 May 2008; accepted 15 September 2008; published online 18 November 2008)

This contribution reports on the development of *in situ* sputter monitoring and end-point detection for ion beam etch systems using continuous-wave cavity ring-down spectroscopy (cw-CRDS). The demonstrated system is based on the detection of sputtered manganese atoms using a tunable external cavity diode laser in the vicinity of 403.07 nm. The cw-CRDS system is described and measurements from a manganese-iron target are presented. End-point detection is demonstrated by monitoring the time dependence of manganese concentration for a multilayer target comprised of alternating layers of manganese/iron and titanium. Detection limits are shown to be adequate for today's commercial ion beam sputter systems. © *2008 American Institute of Physics.*
[DOI: 10.1063/1.2995765]

I. INTRODUCTION

Owing to its unique characteristics, ion beam sputtering (etching) is a preferred method for the manufacture of multilayer structures and coatings for a variety of applications, including dielectric mirrors, thin film heads (TFHs) for data storage, and photovoltaic materials.[1–3] In addition to depositing materials, ion beam etching may be used to form structures in multilayer material stacks. Sensitive and quantitative methods are required for monitoring and process control in industrial etching systems. A particular need in ion beam sputtering systems is end-point detection, i.e., the capability of detecting when a given layer of a multilayer target has been fully etched through (reached its end point) and a new underlying layer has been exposed. Current methods for monitoring and end-point detection are typically based on either optical emission spectroscopy (OES) or secondary ionization mass spectrometry (SIMS). The OES method works well under certain conditions but can suffer from interferences of background beam/plasma interactions within the etch process chamber. The primary shortcoming of the SIMS approach is the relatively high complexity and cost.

Cavity ring-down spectroscopy (CRDS) is a sensitive laser-based absorption technique that has been demonstrated as a sputter diagnostic[4–6] and is potentially suitable for monitoring and end-point detection in commercial ion beam etch systems. Like other laser absorption methods, lower (ground) states are probed so that slight perturbations of the (small) fractions of excited states should not affect signal levels. Relative to conventional laser absorption, CRDS achieves enhanced sensitivity (detection limits of as low as $\sim 10^{-8}$–10^{-11} cm^{-1} for ~ 1 s measurement times) by housing the absorbing species within a high-finesse optical cavity, typically formed from a pair of high-reflectivity mirrors. The probe laser beam is coupled into the optical cavity where it "bounces" back-and-forth many times, e.g., $\sim 10^4$ passes for $R \sim 0.9999$. Ring-down measurements are based on monitoring the exponential decay, $S(t,\upsilon)$, of the light intensity within the cavity,[7,8]

$$S(t,\nu) = S_0 \exp[-t/\tau(\nu)],$$

$$1/\tau(\nu) = \frac{c}{l}\left[\int k(x,\nu)dx + (1-R)\right], \tag{1}$$

where ν is the laser frequency, τ is the $1/e$ time of the decay (termed as the ring-down time), c is the speed of light, l is the cavity length, the x-integration is along the beam within the cavity, k is the absorption coefficient, and $1-R$ is the mirror loss (including scattering and all cavity losses). The path-integrated concentration of absorbing species can be calculated from the change in ring-down time. Owing to the narrower linewidth of continuous-wave (cw) lasers as well as the possibility for higher sampling rates, cw-CRDS[9,10] can provide improved sensitivity as compared to pulsed-CRDS.

II. CRDS SPUTTER MEASUREMENT SYSTEM

The cw-CRDS sputter measurement system is illustrated in Fig. 1. The primary components of the system are an ion sputtering chamber coupled to a cw-CRDS optical detection system. The sputtering facility has been previously described.[4–6] It consists of an ion beam striking a target within a vacuum chamber. A roughing and turbo pumps are used to bring the pressure to approximately 1×10^{-4} Pa under no-flow conditions. With the ion beam operating, the chamber pressure is $\sim 2 \times 10^{-3}$ Pa, so that the sputtered atoms are in a collisionless free-molecular regime (Knudsen number $\ll 1$). A small argon flow (0.4 mg/s) is fed to the system and the ion beam is extracted from an 8 cm diameter ion source.[11]

a)Electronic mail: ayalin@engr.colostate.edu.
b)Visiting scientist at Colorado State University.

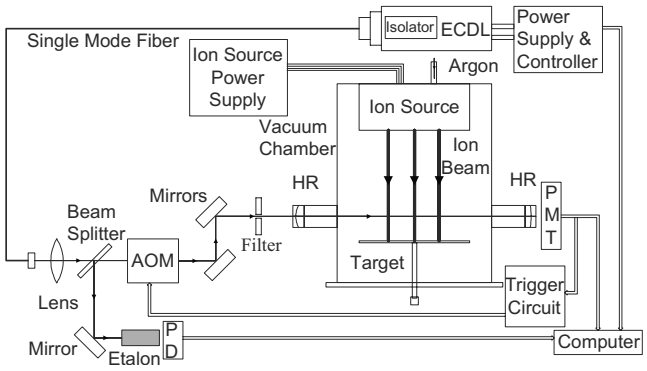

FIG. 1. Schematic of cw-CRDS sputter measurement system. AOM: acousto-optical modulator, PD: photodetector, PMT: photomultiplier tube, HR: high-reflectivity mirror.

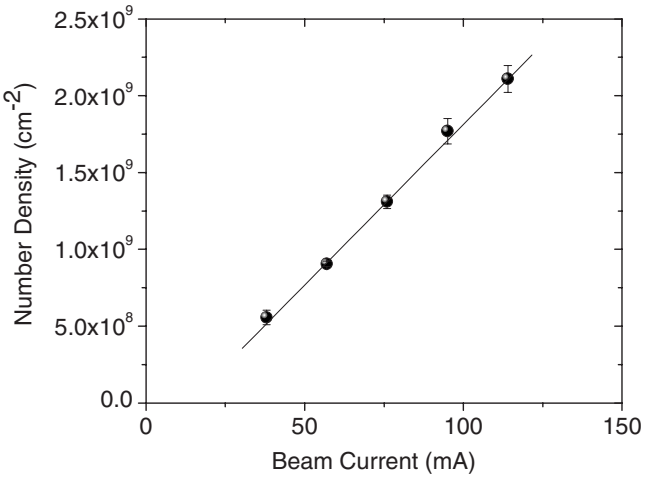

FIG. 2. Dependence of path-integrated manganese number density on the ion beam current.

We use a tunable external cavity diode laser (Toptica DL100) to measure an absorption line of manganese at 403.076 nm (air wavelength). (Manganese is selected owing to its use as a relatively common layer in multilayer TFH structures etched in commercial ion beam etch systems.) The mode-hop free tuning range of the laser is about 30 GHz and the laser linewidth is below 5 MHz. An optical isolator is used to prevent back reflections into the laser. The laser output is delivered to the vicinity of the sputter chamber with a single-mode fiber optic cable. An aspheric lens is used at the fiber exit to collimate the beam and to match the beam to the TEM_{00} mode of the cavity. A photomultiplier tube (PMT) detector is positioned behind the cavity and uses a dielectric interference filter to suppress background light. All measurements are made by scanning the laser wavelength (see below for scan parameters), and ring-down signals are measured each time the laser spectrally overlaps with a cavity transmission peak (so that in a given laser scan the ring-down acquisitions are spaced by the cavity free spectral range). The spectral overlap of laser and cavity yields an increase in the PMT signal which is monitored by a threshold circuit that triggers an acousto-optic modulator (AOM) to extinguish the incoming laser beam. The light in the cavity then exponentially decays, yielding a ring-down event. The ring-down signals are measured with a 20 MHz 12 bit analog-to-digital acquisition board (Adlink PCI-9812/10) connected to a personal computer, and a custom LABVIEW program is used for exponential fitting (with the nonlinear Levenberg–Marquardt fit). A solid etalon (fused silica solid Fabry–Pérot etalon, finesse of ~2 at 390 nm) is used as a frequency reference. The experimental scheme employed here provides sufficient sensitivity and spectral resolution for our purposes. In comparison to methods in which a cavity mirror is scanned on a piezoelectric transducer (PZT), the present method is simpler (and less expensive) as desired for an industrially oriented monitor.

The optical cavity has length of 83 cm and is formed by a pair of high-reflectivity mirrors each 2.54 cm in diameter, with radius of curvature of 1 m. We typically operate with an "empty-cavity ring-down time" of ~20 μs (measured with the etching system operating but the laser detuned) corresponding to $R \sim 99.986\%$. The mirror mounts are mechanically and thermally isolated from the main chamber body by using bellows inline with extender arms. A series of irises (diameter of ~5 mm) is internal to the extender arms and serves to shield the mirrors from deposition of sputtered particles. With this method, minimal degradation of mirror reflectivity has been observed (~5–10 ppm/h), allowing operation for tens of hours with a small sensitivity change. Improved shielding and/or periodic cleaning would be required for longer term operation.

Initial cw-CRDS detection of sputtered manganese (Mn) employed an 8×4 cm^2 Mn/Fe target (50% manganese and 50% iron by mole ratio). The diode laser was set for a 25 GHz mode-hop-free frequency scan every 0.5 s (up-and-down in 1 s). The free spectral range of the 83 cm cavity is approximately 180 MHz so that there are approximately 140 ring-down events (laser/cavity resonances) during each laser scan, corresponding to a ring-down acquisition rate of approximately 280 s^{-1}. The absorption spectrum (and path-integrated number density) of Mn was measured with a normally incident ion beam of 750 eV argon ions. The optical axis was 2 cm above the target. To construct the spectrum we used a binning approach in which the frequency axis was divided into a series of bins, each with width of 1.25 GHz, and signals falling within each bin were averaged (approximately seven signals per bin per scan). The wavelength-integrated area of the spectrum (found by numerical integration) yielded the path-integrated concentration. Figure 2 shows an example of the dependence of the measured Mn concentration on the ion beam current. Concentrations were found every 3 s and the data points shown correspond to the average of multiple measurements (error bar from standard deviation of individual points). The linear density of Mn is proportional to the beam current ($R > 99.8\%$ in the linear fitting) as expected based on operation of this source in this current range. The measured values of Mn concentration compare favorably with simple estimates based on the ion beam current profile, target dimension, and tabulated sputter yields. Data in Fig. 2 were obtained using a honeycomb on the target (to examine the lineshape with reduced lineshape broadening[6]) but the same method is used without the honeycomb.

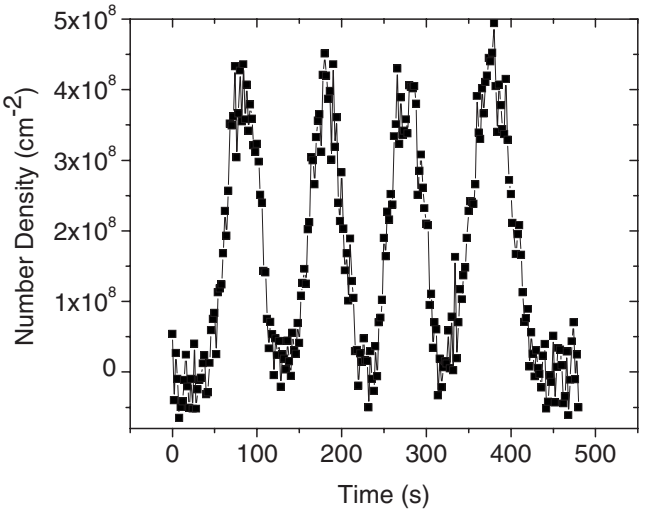

FIG. 3. End-point detection of Mn multilayer target.

III. END-POINT DETECTION

An end-point demonstration based on CRDS detection of Mn is presented in Fig. 3. The measurements employed a multilayer target comprised of alternating layers of Mn/Fe (500 Å thick) and titanium (200 Å). The layers were sputter deposited onto a silicon wafer substrate. A top (outer) layer of titanium (3000 Å) must be sputtered before reaching the alternating layers containing Mn. The dimensions of the target surface were 0.5×0.5 cm^2. The end-point detection was based on measuring the time dependence of path-integrated Mn concentration while the target was etched by the ion beam [as described above and similar to Fig. 2]. We have subtracted a small baseline contribution ($\sim10^8$ cm^{-2}) associated with residual Mn deposited on the vacuum chamber walls and sputtered by divergent ions. (This contribution was present without the target but only when the ion beam is operating.) In this case, the diode laser scan interval was 30 GHz with a scan duration of 1 s (other parameters as above). The ion beam current and voltage were 100 mA and 600 V, respectively.

The cw-CRDS detection system can readily detect the appearance and ending of the Mn-containing layers. The rounded profile of each layer is primarily due to nonuniformity of the ion beam current density. (The nonuniformity leads to varying sputter rates over the target area so that layers start and finish at slightly different times at different locations in the target.) Industrial sources tend to use more spatially uniform ion beams so that relatively clean end points are achieved. The time duration of each Mn/Fe layer is approximately 50 s, corresponding to etching rates of approximately ~10 Å/s for the 500 Å thick layers. The observed etch rates of ~10 Å/s agrees reasonably with a simple numerical estimate of ~15 Å/s based on the average ion current density ($j=1.3$ mA/cm^2), expected sputter yield ($Y=1.51$ atoms/ion based on averaging single-species yields of $Y_{Mn}=2.01$ atoms/ion and $Y_{Fe}=1.00$ atoms/ion for 600 eV argon ions[12]) effective molar mass and density (using average of Mn and Fe values), and the target thickness. The experimental titanium etch rate of ~4 Å/s (~200 Å/50 s) is also reasonably consistent with a similar numerical estimate of etch rate of ~7 Å/s [found analogous to that described above but with titanium properties and $Y_{Ti}=0.53$ atoms/ion (Ref. 12)].

IV. CONCLUSION

The cw-CRDS etch monitor and end-point sensor reported here is, to the best of our knowledge, the first such demonstration. Based on cost and performance, it may represent an industrially attractive method when compared with incumbent techniques. To better gauge practical utility, we consider the detection sensitivity relative to the expected conditions in contemporary ion beam etch systems. Industrial ion beam etch systems typically have sputter (etch) rates of ~100 Å/Min and employ targets with ~10% exposed area corresponding to concentrations of sputtered particles of $\sim10^8$ cm^{-3} (for typical materials). Typical target sizes are ~10–30 cm, corresponding to path-integrated number densities of $\sim10^9$ cm^{-2}. Layer thicknesses are ~10–100 Å so that a measurement rate of ~1 s^{-1} is desired. Relative to these parameters, the demonstrated CRDS monitor is very adequate with detection limit of approximately 3×10^7 cm^{-2} for 1 s measurement times (optical sensitivity of $\sim2\times10^{-9}$ cm^{-1} for 1 s). The high signal-to-noise ratio has enabled unambiguous end-point detection at comparable densities to those in industrial etch systems. Of course, for practical implementation such evaluations would need to be performed for different conditions and species of interest. In comparison to industrial systems, the studies presented here have used higher etch rates but smaller targets. For applications using small features on large substrates, or nonuniform ion beams, the effects of smeared end-point signals need to be examined. If needed, the sensitivity of the cw-CRDS system could be improved by using higher-reflectivity mirrors (commercially available), increasing our sampling rate (e.g., by using a PZT to modulate cavity length), and increasing the laser power or decreasing the laser linewidth (both of which would reduce the detection shot noise). For multispecies detection, a multiplexed approach based on several diode laser heads could be used. Similar implementations could be used for other etching configurations, for example, diode etching.

ACKNOWLEDGMENTS

The authors would like to acknowledge Dan Siegfried (Veeco Instruments, Inc.) for technical discussion and preparation of multilayer targets as well as funding support from Veeco Instruments' Veeco Process Equipment Group (Fort Collins, CO and Plainview, NY).

[1] S. Mohan and M. G. Krishna, Vacuum **46**, 645 (1995).
[2] B. Dieny, J. Magn. Magn. Mater. **136**, 335 (1994).
[3] J.Kelly and R.D.Arnell, Vacuum **56**, 159 (2000).
[4] V. Surla, P. J. Wilbur, M. Johnson, J. D. Williams, and A. P. Yalin, Rev. Sci. Instrum. **75**, 3025 (2004).
[5] A. P. Yalin, V. Surla, M. Butweiller, and J. D. Williams, Appl. Opt. **44**, 6496 (2005).
[6] A. P. Yalin and V. Surla, Opt. Lett. **30**, 3219 (2005).
[7] P. Zalicki and R. N. Zare, J. Chem. Phys. **102**, 2708 (1995).
[8] A. P. Yalin and R. N. Zare, Laser Phys. **12**, 1065 (2002).
[9] D. Romanini, A. A. Kachanov, N. Sadeghi, and F. Stoeckel, Chem. Phys.

Lett. **264**, 316 (1997).
[10] B. A. Paldus, J. S. Harris, Jr., J. Martin, J. Xie, and R. N. Zare, J. Appl. Phys. **82**, 3199 (1997).
[11] W. R. Hudson and B. A. Banks, Proceedings of the Tenth AIAA Electric Propulsion Conference (American Institute of Aeronautics and Astronautics, 1973), AIAA Paper No. 73-1131.
[12] Y. Yamamura and H. Tawara, At. Data Nucl. Data Tables **62**, 181, 188, and 190 (1996).